ANESTHESIOLOGY

Small G-Protein Rheb Gates Mammalian Target of Rapamycin Signaling to Regulate Morphine Tolerance in Mice

Wenying Wang, M.D., Ph.D., Xiaqing Ma, M.D., Ph.D., Wenjie Du, M.D., Raozhou Lin, Ph.D., Zhongping Li, Ph.D., Wei Jiang, M.D., Ph.D., Lu-Yang Wang, Ph.D., Paul F. Worley, Ph.D., Tao Xu, M.D., Ph.D.

ANESTHESIOLOGY 2024; 140:786–802

EDITOR'S PERSPECTIVE

What We Already Know about This Topic

- Analgesic tolerance after chronic administration of morphine involves the activation of the mammalian target of rapamycin pathway in the spinal cord
- Rheb is a GTP-binding protein that modulates mammalian target of rapamycin signaling and plays an important role in the pathogenesis of chronic pain
- The role of the Rheb signaling pathway in morphine-induced tolerance remains unknown

What This Article Tells Us That Is New

- In mice, repeated administration of morphine increased expression of Rheb, leading to activation of mammalian target of rapamycin signaling in the spinal cord
- Genetic overexpression of Rheb impaired morphine analgesia, whereas the deletion of Rheb had opposite effects
- These results suggest that the Rheb–mammalian target of rapamycin signaling pathway plays an important role in the development and maintenance of morphine-induced tolerance

ABSTRACT

Background: Analgesic tolerance due to long-term use of morphine remains a challenge for pain management. Morphine acts on μ-opioid receptors and downstream of the phosphatidylinositol 3-kinase signaling pathway to activate the mammalian target of rapamycin (mTOR) pathway. Rheb is an important regulator of growth and cell-cycle progression in the central nervous system owing to its critical role in the activation of mTOR. The hypothesis was that signaling *via* the GTP-binding protein Rheb in the dorsal horn of the spinal cord is involved in morphine-induced tolerance.

Methods: Male and female wild-type C57BL/6J mice or transgenic mice (6 to 8 weeks old) were injected intrathecally with saline or morphine twice daily at 12-h intervals for 5 consecutive days to establish a tolerance model. Analgesia was assessed 60 min later using the tail-flick assay. After 5 days, the spine was harvested for Western blot or immunofluorescence analysis.

Results: Chronic morphine administration resulted in the upregulation of spinal Rheb by 4.27 ± 0.195-fold ($P = 0.0036$, n = 6), in turn activating mTOR by targeting rapamycin complex 1 (mTORC1). Genetic overexpression of Rheb impaired morphine analgesia, resulting in a tail-flick latency of 4.65 ± 1.10 s ($P < 0.0001$, n = 7) in Rheb knock-in mice compared to 10 s in control mice (10 ± 0 s). Additionally, *Rheb* overexpression in spinal excitatory neurons led to mTORC1 signaling overactivation. Genetic knockout of Rheb or inhibition of mTORC1 signaling by rapamycin potentiated morphine-induced tolerance (maximum possible effect, 52.60 ± 9.56% in the morphine + rapamycin group *vs.* 16.60 ± 8.54% in the morphine group; $P < 0.0001$). Moreover, activation of endogenous adenosine 5′-monophosphate-activated protein kinase inhibited Rheb upregulation and retarded the development of morphine-dependent tolerance (maximum possible effect, 39.51 ± 7.40% in morphine + metformin group *vs.* 15.58 ± 5.79% in morphine group; $P < 0.0001$).

Conclusions: This study suggests spinal Rheb as a key molecular factor for regulating mammalian target of rapamycin signaling.

(ANESTHESIOLOGY 2024; 140:786–802)

Downloaded from http://asa2.silverchair.com/anesthesiology/article-pdf/140/4/786/701885/20240400.0-00022.pdf by guest on 20 March 2024

Supplemental Digital Content is available for this article. Direct URL citations appear in the printed text and are available in both the HTML and PDF versions of this article. Links to the digital files are provided in the HTML text of this article on the Journal's Web site (www.anesthesiology.org).

Submitted for publication February 17, 2023. Accepted for publication December 13, 2023. Published online first on December 26, 2023.

Wenying Wang, M.D., Ph.D.: Department of Anesthesiology, Sixth People's Hospital Affiliated with Shanghai Jiao Tong University School of Medicine, Shanghai, China.

Xiaqing Ma, M.D., Ph.D.: Department of Anesthesiology, Sixth People's Hospital Affiliated with Shanghai Jiao Tong University School of Medicine, Shanghai, China.

Wenjie Du, M.D.: Department of Anesthesiology, Huashan Hospital, Fudan University, Shanghai, China.

Raozhou Lin, Ph.D.: Solomon H. Snyder Department of Neuroscience, Johns Hopkins University School of Medicine, Baltimore, Maryland.

Zhongping Li, Ph.D.: Solomon H. Snyder Department of Neuroscience, Johns Hopkins University School of Medicine, Baltimore, Maryland.

Wei Jiang, M.D., Ph.D.: Department of Anesthesiology, Sixth People's Hospital Affiliated with Shanghai Jiao Tong University School of Medicine, Shanghai, China.

Copyright © 2023 The Author(s). Published by Wolters Kluwer Health, Inc., on behalf of the American Society of Anesthesiologists. This is an open-access article distributed under the terms of the Creative Commons Attribution-Non Commercial-No Derivatives License 4.0 (CCBY-NC-ND), where it is permissible to download and share the work provided it is properly cited. The work cannot be changed in any way or used commercially without permission from the journal. ANESTHESIOLOGY 2024; 140:786–802. DOI: 10.1097/ALN.0000000000004885

The article processing charge was funded by Sixth People's Hospital Affiliated with Shanghai Jiao Tong University School of Medicine.

Chronic pain has emerged as a major public health problem owing to its prevalence and associated excessive use of pain medicine. Population-based estimates of chronic pain among U.S. adults range from 11 to 40%.[1] Opioid analgesics, such as morphine, remain the first line for managing moderate to severe perioperative or chronic pain.[2] However, long-term use of these drugs can result in analgesic tolerance, with analgesic efficacy gradually decreasing at fixed drug doses.[3] The diminished pain control and other adverse effects caused by dose escalation require novel therapeutic strategies to compliment opioid analgesia while mitigating tolerance and hyperalgesia to improve patient safety. Although extensive literature is available on the neurobiological basis of morphine-induced tolerance and hyperalgesia, existing drugs cannot effectively prevent or reverse the occurrence of morphine tolerance, partly because it has a single target. Morphine-induced adaptive processes may be the result of complex alterations at the molecular level,[4] including desensitization, internalization, downregulation, and phosphorylation of opioid receptors or heterodimerization of μ-opioid receptors with other receptors.[5,6] Various mechanisms, such as glutamate receptor activation,[7] descending spinal facilitation,[8,9] activation of glial cells and cytokine release,[10] and protein kinase Cγ and calmodulin-dependent kinase II (CaMKIIα) upregulation in the dorsal horn,[11] have been implicated in analgesic tolerance elicited by the long-term use of morphine.

All of these actions may occur at the translation level. For example, the μ-opioid receptor–triggered mammalian target of rapamycin (mTOR) pathway could promote morphine-induced protein translation in the spinal cord, resulting in morphine tolerance and hyperalgesia.[12] However, the upstream regulatory molecules of mTOR involved in morphine tolerance remain unclear. Rheb (Ras homolog enriched in the brain) is an important regulator of growth and cell-cycle progression in the central nervous system owing to its critical role in the activation of mTOR. Rheb localizes at the lysosome to activate mTOR complex 1 (mTORC1), and Rag7 proteins localize mTORC1 at the lysosome, allowing Rheb to activate the protein.[13] mTOR forms two distinct complexes: mTORC1 and mTORC2. mTORC1 regulates the translation of most proteins by phosphorylated specific downstream effectors, such as the eukaryotic initiation factor 4E–binding proteins and ribosomal S6 protein and is implicated in the regulation of cell growth, proliferation, and cell size. Phosphorylation of Rheb by adenosine 5′-monophosphate–activated protein kinase (AMPK) impairs its nucleotide-binding ability and inhibits Rheb-mediated mTORC1 activation in response to energy depletion.[14] Metformin inhibits the mitochondrial respiratory chain, leading to the activation of AMPK, which enhances insulin sensitivity for type 2 diabetes research. Moreover, metformin can cross the blood–brain barrier and has been implicated in morphine tolerance.[15] Our previous study suggested that spinal Rheb plays a critical role in neuropathic pain; however, the role of the Rheb signaling pathway in morphine-induced tolerance remains unknown.

The spinal dorsal horn is mostly implicated in the generation of opioid tolerance; hence, we postulated that Rheb in the dorsal horn might be a key player in morphine-induced tolerance. Therefore, we investigated the role of the AMPK–Rheb–mTOR signaling axis in the development of morphine analgesic tolerance.

Materials and Methods

Animals

Adult C57BL/6J male and female mice (Animal Center, Chinese Academy of Sciences, Shanghai, China) weighing 20 to 25 g were used in this study. The mice were housed (three to five animals per cage) in a room maintained at a constant ambient temperature of 22 to 23°C and humidity of 50 to 60%, with an alternating 12-h light/12-h dark cycle. Food and water were provided *ad libitum*. All efforts were made to minimize the number of animals used and animal suffering. The animals were randomly assigned to groups using simple randomization, and mice of different groups were cohoused. Age-matched littermates without the *Cre* gene served as control mice in each experiment.

Rheb S16H Conditional Knock-in Mice

Mice with nestin Cre and the *Rheb* S16H knock-in allele were generated in the laboratory of Dr. Worley.[16] The LoxP-flanked tPA (transcriptional stop) was located upstream of the *Rheb* S16H knock-in allele. *Rheb* cDNA transcription started once the floxed tPA (transcriptional stop) was removed by the Cre recombinase and central nervous system–specific knock-in of *Rheb* (*Rheb* knock-in: *Rheb k/k; Nestin cre*) was generated. The genotype of the transgenic mice was determined by PCR using the following primers to distinguish between the wild-type and knock-in allele and cre-mediated excision of the stop signal: WTF1, 5′-GCA CTT GCT CTC CCA AAG TC-3′; WTR1, 5′-GCG GGA GAA ATG GAT ATG AA-3′ to amplify wild-type allele (596 bp); FloxF, 5′-GCA CTT GCT CTC CCA AAG TC-3′; FloxR, 5′-GGG GAA CTT CCT GAC TAG GG-3′ to amplify the knock-in allele (395 bp); 5′-TGC CAC GAC CAA GTG ACA GCA ATG-3′ (forward),

Lu-Yang Wang, Ph.D.: Program in Neuroscience and Mental Health, SickKids Research Institute, Toronto, Ontario, Canada; and Department of Physiology, University of Toronto, Toronto, Ontario, Canada.

Paul F. Worley, Ph.D.: Solomon H. Snyder Department of Neuroscience, Johns Hopkins University School of Medicine, Baltimore, Maryland.

Tao Xu, M.D., Ph.D.: Department of Anesthesiology, Sixth People's Hospital Affiliated with Shanghai Jiao Tong University School of Medicine, Shanghai, China; Department of Anesthesiology, Suzhou Hospital of Anhui Medical University, Suzhou, China; and Solomon H. Snyder Department of Neuroscience, Johns Hopkins University School of Medicine, Baltimore, Maryland.

Downloaded from http://asa2.silverchair.com/anesthesiology/article-pdf/140/4/786/701885/20240400.0-00022.pdf by guest on 20 March 2024

and 5′-ACC AGA GAC GGA AAT CCA TGG CTC-3′ (reverse). The primers generated a 400-bp amplicon and were used for amplification of nestin Cre. Both male and female adult mice were used for behavioral studies.

Establishment of Transgenic Conditional *Rheb* Knockout Mice

Mice with CaMKII cre and loxP-flanked *Rheb* allele were generated in the laboratory of Dr. Worley.[16] Floxed *Rheb* mice were crossed with CaMKII Cre transgenic mice to generate mice with neuron-specific *Rheb* deletion (*Rheb* conditional knockout [cKO]: *Rheb* f/f; CaMKII cre). Genomic DNA was isolated from the ears, and genotyping was performed using the following primers to amplify wild-type (650 bp) and the floxed allele (850 bp): 5′-GCC CAG AAC ATC TGT TCC AT-3′ (forward) and 5′-GGT ACC CAC AAC CTG ACA CC-3′ (reverse). The primers used for the amplification of CaMKII Cre were 5′-GAC AGG CAG GCC TTC TCT GAA-3′ (forward), and 5′-CCT CTC CAC ACC AGC TGT GGA-3′ (reverse), with an amplicon of 500 bp. Both male and female adult mice were used for behavioral studies.

AAV Virus Design

pAAV-CaMKII-GFP-Cre and pAAV-VGAT-EGFP-Cre were obtained from Genechem Company (China). pAAV-CBG-DIO-EGFP-miR30shRNA(Rheb) (target: NM_053075.3) was designed and synthesized by Obio Company (China). AAV9 vector was injected at a maximum feasible dose, with a total volume of 5 μl per animal.

Small Interfering RNA Transfection

An mTOR small interfering RNA (siRNA; catalog no. 6548) and its control scrambled siRNA (catalog no. 6332) were purchased from Cell Signaling Technology Inc. (USA). TurboFect *in vivo* transfection reagent (Thermo Scientific Inc., USA) was used as a delivery vehicle for siRNA to prevent degradation and enhance cell membrane penetration. The mice were injected intrathecally with siRNA or vehicle once daily for 3 days. On day 7, the mice were administered intrathecal injections of saline or morphine, as described below.

Drugs and Groups

Morphine (Shenyang First Pharmaceutical Factory, China) was dissolved in saline at a final concentration of 1 μg/μL. Metformin was purchased from MedChemExpress (USA; catalog no. HY-17471A) and dissolved in saline at a final concentration of 20 μg/μL. Rapamycin (V900930; Sigma–Aldrich, USA) was dissolved in 0.1% dimethyl sulfoxide in saline at a final concentration of 1 μg/μl. All drugs were delivered using an insulin syringe (BD Biosciences, USA). The injection was performed by lumbar puncture into the subarachnoid space of the lumbar thecal at approximately the lumbar 4/5 level, as previously described.[17]

To set the morphine tolerance model, the mice were injected intrathecally with saline (10 μl) or morphine (10 μg/10 μl) twice daily at 12-h intervals for 5 consecutive days. Analgesia was assessed 30 and 60 min later *via* the tail-flick assay.

To determine the analgesic effect of morphine in *Rheb* knock-in mice, nociceptive behavior was examined in the following groups: control with 10 μl of saline, control with 10 μg of morphine, knock-in with 10 μl of saline, and knock-in with 10 μg of morphine. For dose–response analysis, the doses tested were 1, 2, 4, 8, 16, 32, and 64 μg at day 6.

To determine the analgesic effect of morphine in *Rheb* cKO mice, nociceptive behavior was examined in the control with morphine (control + morphine 1 μg) and cKO with morphine (cKO + morphine 1 μg) groups. To determine the development of morphine tolerance in cKO mice, behavioral changes were examined in the following four groups: control with 10 μl of saline, control with 10 μg of morphine, cKO with 10 μl of saline, and cKO with 10 μg of morphine.

To determine the effect of rapamycin on the process of morphine tolerance, vehicle or rapamycin was intrathecally injected 30 min before morphine treatment for 5 days, and the nociceptive behavioral changes were examined in the following groups every single day: 10 μl of saline with 10 μl of vehicle, 10 μl of saline with 10 μg of rapamycin, 10 μg of morphine with 10 μl of vehicle, and 10 μg of morphine with 10 μg of rapamycin. mTOR siRNA (catalog no. 6332) and control scrambled siRNA (catalog no. 6568) were purchased from Cell Signaling Technology Inc. TurboFect *in vivo* transfection reagent (Thermo Scientific Inc.) was used as a delivery vehicle for siRNA to prevent degradation and enhance cell membrane penetration. The mice were injected intrathecally with siRNA or vehicle once daily for 3 days. On day 7, the mice were administered intrathecal injections of saline or morphine as described above. To determine the effect of metformin on the development of morphine tolerance, saline or metformin (200 mg/kg, ip) was administered 30 min before the intrathecal injection of morphine for 5 days, and tail-flick latencies were examined in all groups every day.

Behavioral Nociceptive Tests

The tail-flick test was used to evaluate the antinociceptive effect of the drugs.[18,19] Briefly, the tip of a mouse's tail was submerged into hot water (52.5 ± 0.5°C), and the time until it was lifted from the water was recorded, which was defined as tail-flick latency. To avoid tissue injury, a cut-off time of 10 s was set. Response latencies were recorded three times, with a 10-min interval between each reading. Response latency was measured before (baseline) and at the

Downloaded from http://asa2.silverchair.com/anesthesiology/article-pdf/140/4/786/701885/20240400.0-00022.pdf by guest on 20 March 2024

indicated time after drug administration. All behavioral tests were carried out by a technician who was blinded to the experimental groups.

Western Blotting Analysis

After the behavioral tests, the mice were euthanized under deep anesthesia using pentobarbital (50 mg/kg, ip) infused with ice-cold saline containing heparin, and the lumbar spinal dorsal horn was removed. The spinal dorsal horn was immediately homogenized in an ice-cold tissue protein extraction reagent. The samples were prepared as previously described.[20] The membranes were incubated with the following primary antibodies: mouse anti-Rheb (1:500; Santa Cruz Biotechnology, USA), mouse anti-actin (1:1,000; Cell Signaling Technology), rabbit anti-p-mTOR-Ser^{2448} (1:1,000; Cell Signaling Technology), rabbit anti-mTOR (1:1,000; Cell Signaling Technology), rabbit anti-p-S6-Ser$^{235/236}$ (1:1,000; Cell Signaling Technology), rabbit anti-S6 (1:1,000; Cell Signaling Technology), rabbit anti-*P*-4E-BP1-Thr$^{37/46}$ (1:1,000; Cell Signaling Technology), rabbit anti-4E-BP1 (1:1,000; Cell Signaling Technology), rabbit anti-p-AMPKα1-Thr^{183}/ AMPKα2-Thr^{172}(1:1,000, Abcam, USA), and rabbit anti-AMPK (1:1,000; Abcam, USA) at 4°C overnight. The blots were washed in Tris-buffered saline with Tween 20 and incubated with secondary antibodies (1:5,000; Huaan Biotechnology, China). Signals were detected by Image Quant Ai600 (General Electric Co., USA) using an enhanced chemiluminescence reagent (Thermo Fisher Scientific, USA) and visualized with the ChemiDocXRS system (Bio-Rad, USA). The results were analyzed and quantified using ImageJ software (version 2.0.0; National Institutes of Health, USA).

Fluorescence Immunohistochemistry and Image Analysis

The mice were transcardially perfused first with cold saline, followed by 4% cold paraformaldehyde under deep anesthesia. The lumbar spinal cord was harvested, postfixed with 4% paraformaldehyde for 4 h, and dehydrated overnight in sucrose at 4°C. Frozen sections (10 μm) were cut on microscope slides before further detection. Double staining was used to identify the colocalization of pS6 with Rheb; pS6 and Rheb with NeuN, CD11b, or Iba1; and GFAP and pS6 with GAD67 and VGLUT2 in the spinal cord. The slides were incubated overnight with primary antibodies (rabbit anti-pS6, 1:500, Cell Signaling Technology; mouse anti-Rheb, 1:50, Santa Cruz; rabbit anti-NeuN, 1:1,000, Huaan; mouse anti-NeuN, 1:1,000, Thermo Fisher; mouse anti-CD11b, 1:100, Abcam; rabbit anti-Iba1, 1:200, Huaan; mouse anti-GFAP, 1:200, Abcam; rabbit anti-GFAP, 1:200, Huaan; rabbit anti-GAD67, 1:200, Abcam; and rabbit anti-VGLUT2, 1:200, Abcam). On the second day, the slides were washed in phosphate-buffered saline and incubated with the following secondary antibodies for 2 h at 25 ± 1°C: goat anti-rabbit IgG H&L, Alexa Fluor 594, 1:500, Abcam; goat anti-mouse IgG H&L, Alexa Fluor 594, 1:500, Abcam; goat anti-mouse IgG H&L, Alexa Fluor 488, 1:500, Abcam; goat anti-mouse IgG H&L, and Alexa Fluor 488, 1:500, Abcam). Images were acquired using a fluorescence microscope (DM IL LED; Leica, USA).

Electrophysiologic Recording

Spinal cord slices were prepared as described previously.[21] The mice (postnatal days 15 to 25) were anesthetized with pentobarbital (50 mg/kg, ip); the spinal cords were rapidly excised and placed in ice-cold cutting solution containing the following and oxygenated with 95% O_2 and 5% CO_2 (310 to 320 mOsm): 95 mM NaCl, 1.8 mM KCl, 1.2 mM KH_2PO_4, 7 mM $MgSO_4$, 0.5 mM $CaCl_2$, 26 mM $NaHCO_3$,50 mM sucrose, and 15 mM glucose (pH 7.4). Transverse slices (300 μm) were cut from the lumbar spinal cord using a vibratome (VT1200; Leica, Germany). The slices were incubated in artificial cerebrospinal fluid containing the following: 127 mM NaCl, 1.8 mM KCl, 1.3 mM $MgSO_4$, 1.2 mM KH_2PO_4,2.4 mM $CaCl_2$, 26 mM $NaHCO_3$, and 15 mM glucose, followed by bubbling with 95% O_2 and 5% CO_2 (310 to 320 mOsm) for 40 min at 34°C. The slices were transferred to a recording chamber and continuously perfused with oxygenated artificial cerebrospinal fluid at a rate of 3 ml/min (22 to 26°C).

Whole-cell patch-clamp recordings were acquired using an EPC-10 triple amplifier (HEKA, German), and the signals were filtered at 2.9 kHz and sampled at 15 kHz. The recording micropipettes were made from borosilicate glass capillaries (Sutter, USA) and had a resistance of 5 to 8 MΩ. The internal solution contained the following: 3 mM Na_2ATP, 125 mM potassium gluconate, 0.5 mM NaGTP, 2 mM $CaCl_2$, 2 mM $MgCl_2$, 10 mM HEPES, and 10 mM EGTA (pH 7.5). Neurons were randomly picked from the laminae II of the dorsal horn.

Statistics

No statistical analyses were used to predetermine the sample size; however, our sample sizes were based on a previous report.[22] At least four animals were used for each recording protocol. Data on behavioral tests were converted to a percentage maximum possible effect calculated as follows: the percentage maximum possible effect = 100 × (post-drug latency threshold – predrug latency threshold)/(cut-off latency threshold – pre-drug latency threshold). The relative expression of proteins was normalized to that of β-actin in different groups, and the phosphorylation levels were compared with the total level of target proteins. The data are presented as means ± SD. Statistical analysis was performed using GraphPad Prism 9 (GraphPad Software Inc., USA). The investigators performing the behavioral, cell counting, protein quantitation, and electrophysiologic experiments

Downloaded from http://asa2.silverchair.com/anesthesiology/article-pdf/140/4/786/701885/20240400.0-00022.pdf by guest on 20 March 2024

were blinded to the treatment and genotypes. Outliers were not evaluated, and no data were excluded from statistical analyses. Before analysis, all data were tested using the Shapiro–Wilk normal distribution test. Parametric tests or nonparametric tests were used according to the results of the normal distribution tests. All statistical analyses were two-tailed. Unpaired Student's *t* tests were used to compare differences between two groups. Multiple group comparisons were performed using one-way or two-way ANOVA with mix design or repeated measures followed by Bonferroni's post-tests. Statistical significance was set at $P < 0.05$.

Study Approval

The animal experiments were in compliance with the guiding principles of the Care and Use of Animals and the Animal Management Rule of the Ministry of Public Health, People's Republic of China (document No. 545, 2001), and were approved by the Animal Care and Use Committee of the Sixth People's Hospital Affiliated with Shanghai Jiao Tong University (document No. SYXK-2016-0020). All the transgenic mice were provided by Dr. Paul Worley and transported from his lab to Dr. Xu's lab in Shanghai by World Courier under suitable conditions: less than three males or five females per cage at a constant ambient temperature of 22 to 23°C. Food and water were provided *ad libitum*.

Results

Spinal Rheb Regulates Acute Morphine Efficacy and Tolerance through mTOR Signaling

To explore the role of Rheb in acute antinociception and chronic morphine tolerance using 1- and 5-day treatments (fig. 1, A and C), we tested whether *Rheb* overexpression or conditional knockout affects morphine-induced acute antinociception or chronic tolerance. To overexpress *Rheb*, we utilized Rosa26-*Rheb* S16H transgenic mice (*Rheb* knock-in),[13] the establishment of which was validated *via* PCR (Supplemental Content 1A, https://links.lww.com/ALN/D418). The *Rheb* knock-in mice exhibited a 3.47 ± 0.883-fold overexpression of spinal Rheb (Supplemental Content 1B, https://links.lww.com/ALN/D418; $P = 0.001$, n = 6) and significant phosphorylated levels of mTOR by 1.879 ± 0.392-fold ($P = 0.0012$), S6 by 1.553 ± 0.274-fold ($P = 0.0011$), and 4EBP1 by 2.445 ± 0.724-fold ($P = 0.0009$; Supplemental Content 1C, https://links.lww.com/ALN/D418; n = 6), indicating persistent activation of mTORC1 signaling. Regarding tail withdrawal latency from warm water, morphine-induced antinociception after intrathecal injection was impaired in *Rheb* knock-in mice (fig. 1B, left panel, tail-flick latency: 4.65 ± 1.10 s in *Rheb* knock-in mice *vs.* 10 ± 0 s in littermate control mice, means ± SD, $P < 0.0001$, n = 7), with an efficacy of 42.66% compared to the control group (fig. 1B, right panel, maximum possible effect: 100% in control mice *vs.* 42.66 ± 11.46% in *Rheb* knock-in mice, $P < 0.0001$, n = 7). During the revision of the article, as per editorial request to investigate sex as a biologic variable, we performed these experiments in female mice and obtained similar results (Supplemental Content 2A and 2B, https://links.lww.com/ALN/D418, tail-flick latency: 4.62 ± 0.73 s in *Rheb* knock-in mice *vs.* 9.05 ± 0.45 s in littermate control mice, $P < 0.0001$; maximum possible effect: 89.42 ± 4.93% in control mice *vs.* 4.98 ± 8.00% in *Rheb* knock-in mice, $P < 0.0001$, n = 6).

To investigate the effects of *Rheb* knockout on morphine-induced chronic tolerance, we crossed floxed *Rheb* mice with CaMKII-Cre transgenic mice to generate central nervous system–specific deletion of *Rheb* (*Rheb* cKO, Supplemental Content 1D, https://links.lww.com/ALN/D418). Immunoblotting analysis using total proteins showed that Rheb levels in the spinal cord (Supplemental Content 1E, https://links.lww.com/ALN/D418, Rheb level: 0.81 ± 0.27 in control mice *vs.* 0.15 ± 0.08 in *Rheb* cKO mice, $P = 0.0001$, n = 6) were significantly lower in *Rheb* cKO mice than in control mice, which indicated that Rheb was successfully deleted in *Rheb* cKO mice. We first determined whether the morphine tolerance model was successfully established in wild-type control and *Rheb* cKO mice. Thermal nociceptive thresholds were measured 1 h after each daily injection to evaluate tolerance. Consistent with our previous work,[23] we found that in wild-type mice, chronic morphine treatment produced significant antinociceptive tolerance (Supplemental Content 3A and 3B, https://links.lww.com/ALN/D418; maximum possible effect: 99.04 ± 1.66% on day 1 *vs.* 15.58 ± 5.79% on day 5, $P < 0.0001$, n = 6) with a fixed twice daily dose of 10 μg, which significantly upregulated the excitability of spinal neurons (fig. 2, A to G; saline + vehicle *vs.* morphine + vehicle). Remarkably, we observed that while morphine antinociception progressively diminished in littermate controls, morphine retained nearly full antinociceptive efficacy across all days in *Rheb* cKO mice (fig. 1D). Morphine-induced antinociception in *Rheb* cKO mice decreased gradually similar to that in the littermate control during the 5-day treatment course; notably, the *Rheb* cKO group retained a substantially higher sensitivity to morphine-induced antinociception than the control group (fig. 1, E and F, maximum possible effect on day 5: 16.13 ± 6.16% in control mice *vs.* 49.08 ± 6.32% *Rheb* cKO mice, $P < 0.0001$; change in maximum possible effect: −82.81 ± 5.62% in control mice *vs. Rheb* cKO mice −48.16 ± 9.13% *Rheb* cKO mice, $P < 0.0001$, n = 6). These results demonstrate that Rheb, through gain and loss of function, bidirectionally controls nociception and its adaptation to morphine, highlighting its critical role in spinal cord nociception processing. Similar results were observed in female mice (Supplemental Content 2, C–E, https://links.lww.com/ALN/D418; maximum possible effect on day 5: 23.51 ± 5.99% in control mice *vs.* 54.15 ± 7.96% in *Rheb* cKO mice, $P < 0.0001$; change in maximum possible

Downloaded from http://asa2.silverchair.com/anesthesiology/article-pdf/140/4/786/701885/20240400.0-00022.pdf by guest on 20 March 2024

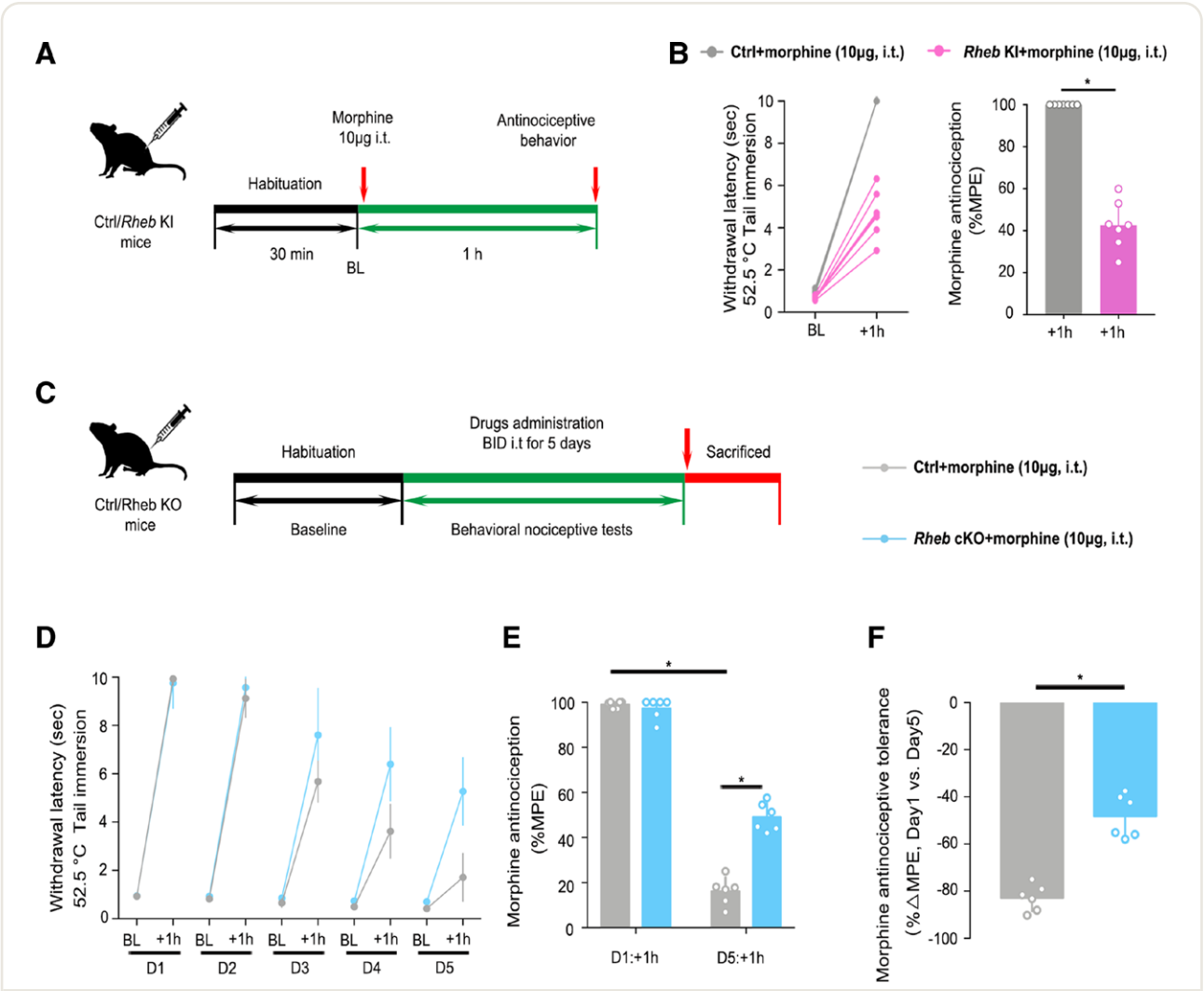

Fig. 1. Modulation of spinal Rheb expression affects acute morphine efficacy and the development of morphine-induced tolerance in male mice. (*A*) Timeline of the experimental procedure. (*B*) Nociceptive behavior (premorphine baseline [BL] time points) and morphine antinociception (postmorphine + 1-h time points) from the first administration (10 μg in 10 μl of saline, intrathecal) in *Rheb* S16H mice (*left*). Shown is the maximum possible effect (MPE) for morphine antinociception from the first administration in *Rheb* S16H mice (*right*; n = 7 mice in each group). (*C*) Establishment of morphine-induced tolerance control (Ctrl)/*Rheb* conditional knockout [cKO] mouse model. (*D*) Daily nociceptive behavior and morphine antinociception during a 5-day chronic morphine schedule (10 μg in 10 μl of saline, intrathecal, twice daily; n = 6 mice in each group). (*E*) MPE for morphine antinociception from the first administration (day 1, + 1 h) compared to the last administration (day 5, + 1 h). (*F*) Percentage of change for each subject. The data are presented as means ± SD by unpaired two-tailed Student's t test (*B*, *F*) or repeated-measures two-way ANOVA + Bonferroni (*D*, *E*). **P* < 0.05. The overlaid points are individual animal scores. BL, baseline; +1 h, 1 h after morphine injection; D1, on Day 1.

effect: −71.44 ± 6.61% in control mice *vs.* −42.02 ± 9.68% in *Rheb* cKO mice, $P = 0.0001$, n = 6).

Chronic Morphine Treatment Increases *Rheb* Expression in Excitatory Neurons in the Spinal Dorsal Horn

Because modulation of *Rheb* affected the analgesic effect of acute morphine and the development of morphine-induced tolerance, we examined the functional impact and Rheb expression in the spinal cord after the establishment of morphine tolerance. After 5 days of morphine administration, the mice were euthanized for immunohistochemistry analyses. The mRNA level of Rheb did not increase after chronic morphine treatment (fig. 3, A and B, Rheb mRNA level: 1.7 ± 0.30 in saline group *vs.* 1.348 ± 0.1052 in morphine group, $P = 0.3011$, n = 6); however, there was significant increase in the protein level by 4.27 ± 0.195-fold (fig. 3C, $P = 0.0036$, n = 6) and fluorescent immunoreactivity of Rheb (fig. 3D, Rheb positive cells percentage: 19.50 ± 0.4.18% in saline group *vs.* 63.67 ± 12.55% in morphine group, $P < 0.0001$, n = 6) in the spinal dorsal horn of mice that received morphine treatment.

Downloaded from http://asa2.silverchair.com/anesthesiology/article-pdf/140/4/786/701885/20240400.0-00022.pdf by guest on 20 March 2024

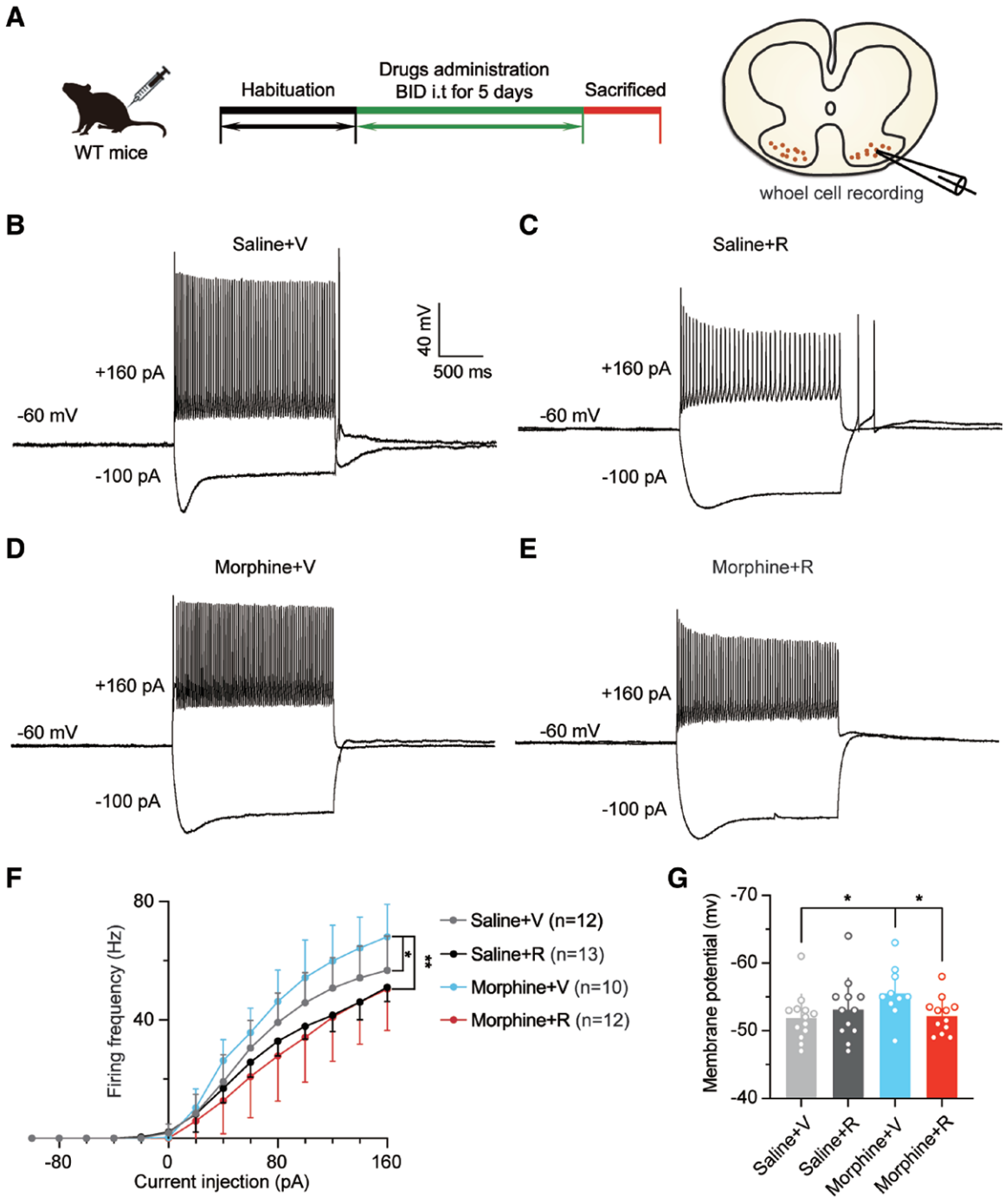

Fig. 2. Blocking spinal mTORC1 decreases chronic morphine-induced increase in neuronal firing rates in the spinal dorsal horn. (*A*) Timeline of the experimental procedure. (*B*, *C*) Representative traces showing dorsal horn neuron voltage responses evoked by current injections (–100 pA, 160 pA) in control mice after 5 days of continuous application of vehicle (V; *B*) or rapamycin (R; *C*). (*D*, *E*) Representative traces showing dorsal horn neuron voltage responses evoked by current injection (–100 pA, 160 pA) in control mice after 5 days of continuous application of morphine (*D*) or morphine and rapamycin (*E*). (*F*) Summary of data showing the effect of current injection evoked spike firing after application of saline or rapamycin. (*G*) Summary of data showing the resting membrane potential in four groups (n = 12 for the saline + V group; n = 13 for the saline + R group; n = 10 for the morphine + V group; n = 12 for the morphine + R group). The two-way mixed-effects ANOVA was performed for the data in panel *F*, and unpaired Student's *t* test was performed for the data in panel *G*. The data are presented as means ± SD. $^{*}P < 0.05$; $^{**}P < 0.01$.

Downloaded from http://asa2.silverchair.com/anesthesiology/article-pdf/140/4/786/701885/20240400.0-00022.pdf by guest on 20 March 2024

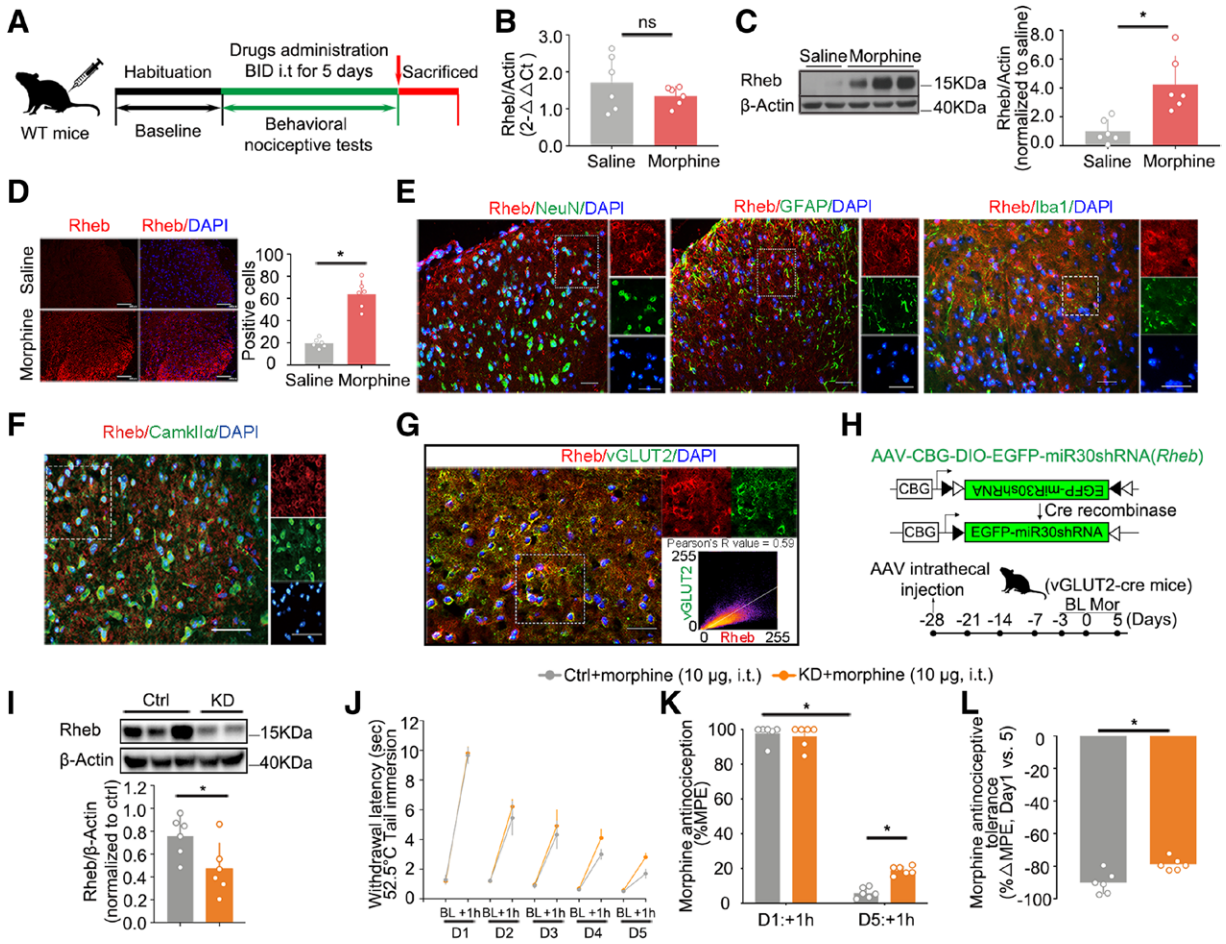

Fig. 3. Chronic morphine treatment increases Rheb expression in excitatory neurons in the spinal dorsal horn. (*A*) Establishment of morphine-induced tolerance in a wild-type (WT) mouse model. (*B*) Expression of *Rheb* in the spinal dorsal horn. (*C*) Immunoblotting of the spinal dorsal horn with anti-Rheb antibodies. (*D*) Immunostaining of the spinal dorsal horn with anti-Rheb antibodies. Representative images of at least six experiments are displayed. *Scale bars*, 20 μm. (*E*) Immunofluorescence double labeling of Rheb (*red*) with NeuN (*green*, *left*), GFAP (*green*, *middle*), and Iba1 (*green*, *right*) in the spinal dorsal horn. *Scale bars*, 20 μm. (*F*) Immunofluorescence double staining of Rheb (*red*) with CaMKIIα (*green*). *Scale bars*, 20 μm. (*G*) Immunofluorescence double labeling of Rheb (*red*) with excitatory neuronal marker vGLUT2 (*green*) in the spinal dorsal horn. The Pearson's *R* value of colocalization was quantified. *Scale bars*, 20 μm. (*H*) Scheme for genetic lesions of vGLUT2 Cre neurons in the spinal dorsal horn and protocol for the experiments. (*I*) Knockdown (KD) of *Rheb* was confirmed by immunoblotting. (*J*) Daily nociceptive behavior and morphine antinociception during a 5-day chronic morphine schedule of vGLUT2 Cre mice injected with *Rheb* shRNA AAV or control AAV. (*K*) Antinociceptive tolerance: maximum possible effect (MPE) for morphine antinociception from the first administration (day 1, + 1 h) compared to the last administration (day 5, + 1 h). (*L*) Percentage of change in each subject (n = 6 mice in each group). The data are presented as means ± SD by unpaired two-tailed Student's *t* test (*B*, *C*, *D*, *I*, *L*) or repeated-measures two-way ANOVA + Bonferroni (*K*). **P* < 0.05. The overlaid points are individual animal scores. BL, baseline; +1 h, 1 h after morphine injection.

To map out the neuronal population expressing increased levels of Rheb, we performed immunolabeling experiments with the neuronal marker NeuN, astrocyte marker GFAP, and microglia marker Iba1 (fig. 3E). Rheb was expressed predominantly in neurons and astrocytes, but not in microglia. Moreover, double-staining experiments of Rheb with vGLUT2 (fig. 3F) and CaMKIIα (fig. 3G) showed that Rheb was expressed in excitatory neurons in the spinal cord.

To determine the role of spinal Rheb in the development of morphine tolerance, we intrathecally injected *Rheb* shRNA AAV into vGLUT2 Cre mice to generate spinal cord–specific *Rheb* knockdown from the excitatory neurons to rule in or out potential contributions of other central excitatory neurons (fig. 3H). The efficiency of *Rheb* knockdown was confirmed by immunoblotting (fig. 3I, Rheb level: 0.76 ± 0.18 in control mice *vs.* 0.47 ± 0.23 in knockdown mice, $P = 0.03$, n = 6). The excitatory neuron-specific *Rheb* knockdown mice were resistant to morphine-induced chronic tolerance (fig. 3, J to L; maximum possible effect on day 5: 5.98 ± 2.97% in control mice

Downloaded from http://asa2.silverchair.com/anesthesiology/article-pdf/140/4/786/701885/20240400.0-00022.pdf by guest on 20 March 2024

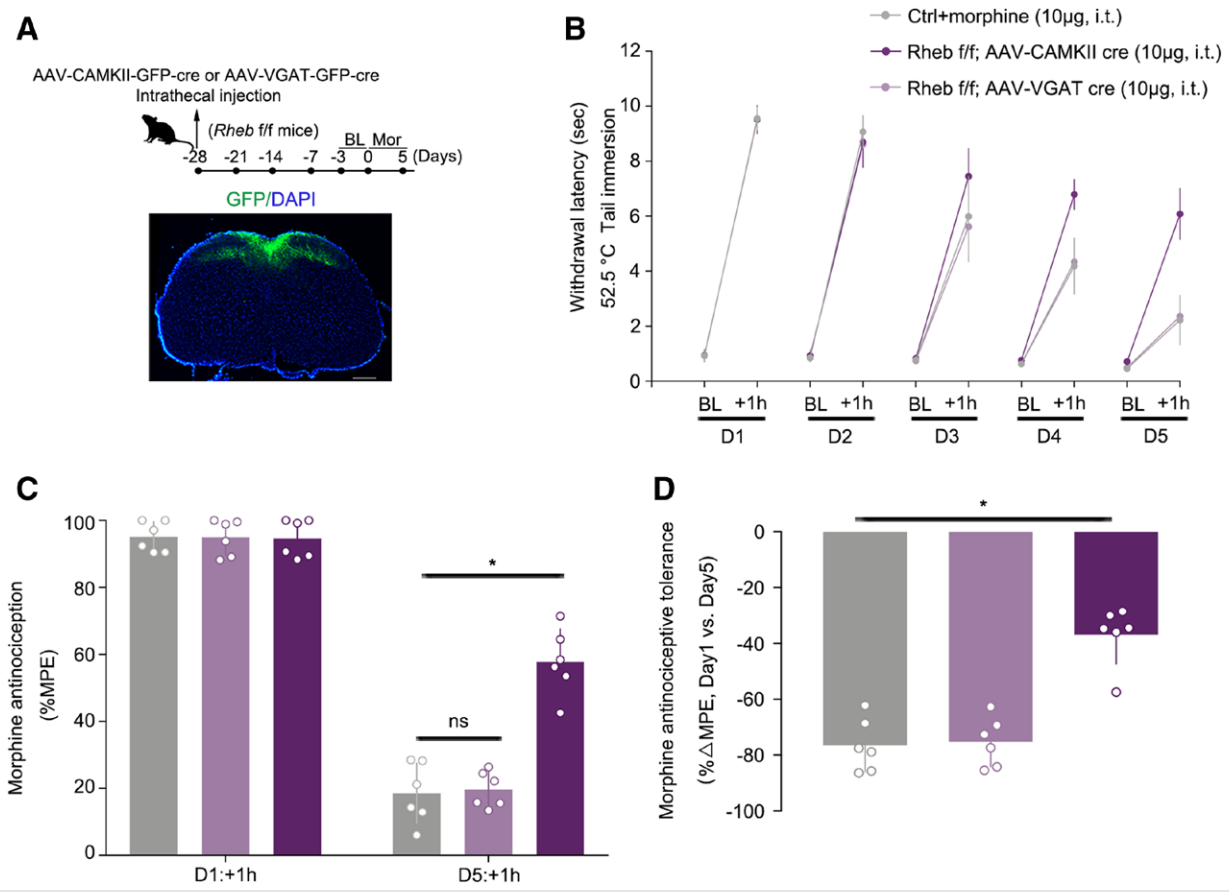

Fig. 4. Rheb knockdown in excitatory neurons in the spinal dorsal horn prevents morphine-induced tolerance. (*A*) Protocol for the experiments and verification of Cre virus expression in the spinal cord. (*B*) Daily nociceptive behavior and morphine antinociception during a 5-day chronic morphine schedule of Rheb flox/flox (f/f) mice injected with *CaMKII-Cre* or *VGAT-Cre* AAV or Rheb flox/flox control mice. (*C*) Antinociceptive tolerance: maximum possible effect (MPE) for morphine antinociception from the first administration (day 1, + 1 h) compared to the last administration (day 5, + 1 h). (*D*) Percentage of change in each subject (n = 6 mice in each group). The data are presented as means ± SD by repeated-measures two-way ANOVA + Bonferroni (*C*) or one-way ANOVA + Bonferroni (*D*). **P* < 0.05. The overlaid points are individual animal scores. BL, baseline; +1 h, 1 h after morphine injection; D1, on Day 1.

vs. 18.94 ± 2.48% in *Rheb* knockdown mice, $P = 0.0001$; change in maximum possible effect: −90.11 ± 6.90% in control mice *vs.* −78.82 ± 3.82% in *Rheb* knockdown mice, $P = 0.0049$, n = 6). These results demonstrate that Rheb upregulation in excitatory neurons is causally linked to the development of morphine tolerance.

Because CaMKII-Cre-mediated manipulation is not restricted to the spinal cord, we further introduced CaMKII-Cre and VGAT-Cre viruses to the sacral spinal cord of Rheb flox/flox mice to specifically knock down Rheb in excitatory and inhibitory neurons, respectively, to assess which type of neuron is involved in mediating morphine tolerance. Figure 4A shows a schematic diagram of the experimental procedure and successful expression of the Cre virus in the spinal dorsal horn. Surprisingly, only Rheb f/f;CaMKII-Cre mice, but not Rheb f/f;VGAT-Cre mice, delayed the occurrence of morphine tolerance (fig. 4, B to D; maximum possible effect on day 5: 18.53 ± 8.99% in control mice *vs.* 57.78 ± 9.87% in Rheb f/f;CaMKII-Cre mice, $P < 0.0001$; change in maximum possible effect: −76.54 ± 9.54% in control mice *vs.* −38.84 ± 10.53% in Rheb f/f;CaMKII-Cre mice, $P < 0.0001$, n = 6). These data further indicate that Rheb, specifically in spinal excitatory neurons, plays an important role in morphine tolerance.

Rheb Stimulates mTORC1 Signaling in Excitatory Neurons in the Spinal Dorsal Horn to Promote Morphine Tolerance

Located downstream of Rheb, the mTOR signaling pathway has been previously implicated in various functions, such as cell growth and proliferation and synaptic plasticity.[24–26] Inhibition of mTOR by rapamycin has resulted

Downloaded from http://asa2.silverchair.com/anesthesiology/article-pdf/140/4/786/701885/20240400.0-00022.pdf by guest on 20 March 2024

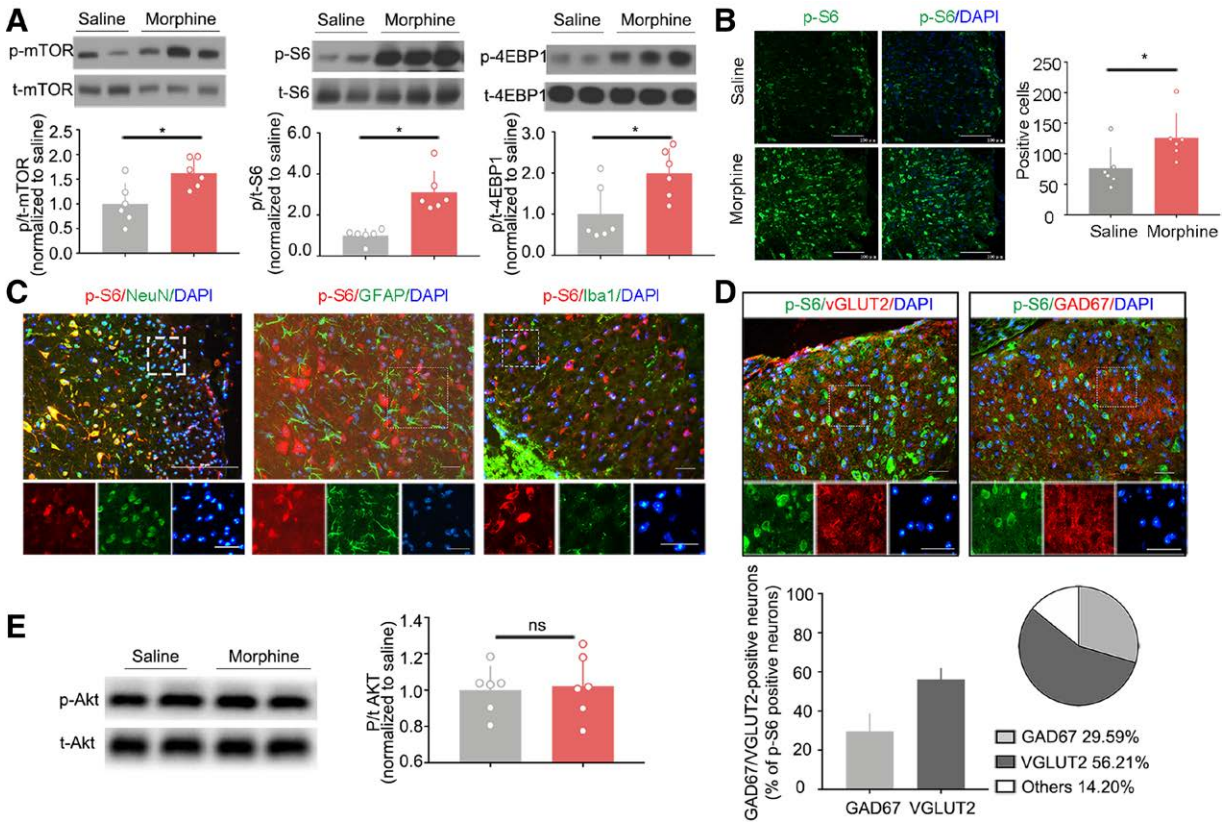

Fig. 5. Chronic morphine treatment increases expression of mTORC1 signaling in excitatory neurons in the spinal dorsal horn. (*A*) Immunoblotting of spinal dorsal horn with anti-p/t-mTOR, p/t-4EBP1, and p/t-S6 antibodies in mice administered with saline and morphine. (*B*) Immunostaining of spinal dorsal horn with anti-p-S6 antibodies. Representative images of at least six experiments are displayed. *Scale bars*, 20 μm. (*C*) Immunofluorescence double labeling of p-S6 (*red*) with NeuN (*green*, *left*), GFAP (*green*, *middle*), and Iba1 (*green*, *right*) in the spinal dorsal horn. *Scale bars*, 20 μm. (*D*) Immunofluorescence double labeling of p-S6 (*green*) with excitatory neuronal marker vGLUT2 (red) and inhibitory neuronal marker GAD67 (*red*) in the spinal dorsal horn. The *top image* is enlarged in three separate boxes with single and merged images included in the picture. *Scale bars*, 50 μm (*top*), 20 μm (*bottom*). The proportion of spinal vGLUT2$^+$ and GAD67$^+$ neurons with p-S6 expression (n = 4 to 6 per group) is shown. (*E*) Immunoblotting of spinal dorsal horn with anti-p-AKT (Ser473) in mice administered with saline and morphine (n = 6 mice in each group). The data are presented as means ± SD by unpaired two-tailed Student's *t* test (*A*, *B*, *D*, *E*). **P* < 0.05. The overlaid points are individual animal scores.

in autophagy upregulation, reduced neuroinflammation, a neuroprotective effect in multiple neurodegenerative disorders, and a potent immunosuppressant effect.[27,28]

Consistent with previous research,[12] repeated morphine treatment induced mTORC1 activation (fig. 5A), as evidenced by significant phosphorylation of spinal mTOR (phosphorylation level: 1 ± 0.42 in saline group *vs.* 1.63 ± 0.29 in morphine group, $P = 0.0133$, n = 6), 4EBP1 (phosphorylation level: 1 ± 0.69 in saline group *vs.* 1.99 ± 0.59 in morphine group, $P = 0.0235$, n = 6), and S6 (phosphorylation level: 1 ± 0.33 in saline group *vs.* 3.11 ± 1.01 in morphine group, $P = 0.0006$, n = 6) after the establishment of morphine tolerance. Increased immunoreactivity of p-S6 was detected in the spinal dorsal horn of mice after chronic morphine treatment (fig. 5B); however, mTORC2 signaling remained unaffected (fig. 5E; phosphorylation level: 1 ± 0.13 in saline group *vs.* 1.02 ± 0.18 in morphine group, $P = 0.808$, n = 6). These data confirmed that chronic morphine-induced tolerance results in the spinal activation of mTORC1 signaling but not mTORC2.

We examined the localization of p-S6 in different neuronal cell types. Chronic morphine-induced p-S6 was mainly localized in the neurons but not in the astrocytes or microglia (fig. 5C). To identify the specific subset of neurons that are involved in chronic morphine-induced mTORC1 signaling, we investigated the portion of p-S6 expressed in excitatory and inhibitory neurons in the spinal dorsal horn. Double-immunofluorescence staining results showed a strong overlap of p-S6 with vGLUT2 (percentage, 56.21 ± 5.53%), a specific excitatory neuronal marker, and partial colocalization with GAD67 (percentage, 29.59 ± 8.96%), a specific inhibitory neuronal marker (fig. 5D; $P = 0.0008$, n = 6). These overlapping expression patterns indicate that chronic

Downloaded from http://asa2.silverchair.com/anesthesiology/article-pdf/140/4/786/701885/20240400.0-00022.pdf by guest on 20 March 2024

morphine-induced Rheb expression and the activation of mTORC1 signaling occurred in the same neurons.

We intrathecally injected rapamycin,[29] an inhibitor of mTOR activity, to observe its effect on the development of morphine-induced tolerance. During the development of morphine-induced tolerance, the reduction in morphine-induced antinociceptive effect was significantly mitigated by coadministration of rapamycin (fig. 6A), retaining approximately 50% of the maximum possible effect on day 5 in the morphine + rapamycin group compared to the morphine + vehicle group (fig. 6B; maximum possible effect on day 5: 52.60 ± 9.56% in morphine + rapamycin group *vs.* 16.60 ± 8.54% in morphine + vehicle group, $P < 0.0001$, $n \geq 4$). The maximum possible effect on day 5 was reduced to approximately 80% in the morphine group compared to that on day 1, and coadministration of rapamycin partially prevented the decrease, resulting in 40% of morphine-induced maximum possible effect (fig. 6C; change in maximum possible effect: −41.91 ± 10.63% in morphine + rapamycin group *vs.* −79.98 ± 6.17% morphine + vehicle group, $P < 0.0001$, $n \geq 4$). Moreover, coadministration of rapamycin significantly blocked the rightward shift of the dose–response curve caused by chronic morphine treatment (fig. 6D), with a lower EC_{50} (3.617 μg) in the morphine + rapamycin group than in the vehicle group (9.145 μg) on day 6 (fig. 6E; $P < 0.0001$, $n = 6$). To further enhance the activity of spinal mTOR, we knocked down mTOR with intrathecal mTOR siRNA. In mice treated with mTOR siRNA, mTOR expression was specifically and selectively reduced compared with saline-treated controls (fig. 6, F and G; mTOR level: 0.98 ± 0.23 in saline + vehicle group *vs.* 0.34 ± 0.05 in saline + siRNA group, $P < 0.0001$; 1.18 ± 0.15 in morphine + siRNA scramble group *vs.* 0.34 ± 0.05 in morphine + siRNA group, $P < 0.0001$, $n = 6$). Similar to rapamycin, mTOR siRNA substantially prevented the morphine-induced rightward shift of the dose–response curve (fig. 6H), and the EC_{50} in mTOR siRNA group (3.678 μg) was much lower than that in the scrambled mTOR siRNA group (7.814 μg). Vehicle and scrambled mTOR siRNA had no effect on spinal mTOR expression or morphine-induced tolerance. To investigate the neural excitability before and after rapamycin treatment, we performed whole-cell patch-clamp recordings in laminae II dorsal horn neurons (fig. 2A). Rapamycin effectively prevented morphine-induced upregulation of firing evoked by current injection (fig. 2, B to F; saline + vehicle *vs.* morphine + vehicle: $P = 0.0461$; morphine + vehicle *vs.* morphine + rapamycin: $P = 0.0018$) and resting membrane potential in the spinal dorsal horn neurons (fig. 2G; saline + vehicle *vs.* morphine + vehicle: 51.90 ± 3.51 *vs.* 55.58 ± 3.85, $P = 0.0263$; morphine + vehicle *vs.* morphine + rapamycin: 55.58 ± 3.85 *vs.* 52.21 ± 2.68, $P = 0.0252$). These results suggest that inhibition of spinal mTOR signaling can attenuate morphine-induced tolerance. Collectively, our results indicate that chronic morphine-induced tolerance was dependent on Rheb and activation of mTORC1 signaling in spinal excitatory neurons, implicating their roles in priming the developmental trajectories of morphine tolerance.

Metformin Prevents Opiate Tolerance by Preventing Rheb Induction

Our results thus far have demonstrated that Rheb upregulation is related to the development of morphine-induced tolerance through mTORC1 activation, prompting us to explore related upstream signaling mechanisms. Previous studies suggest that as a negative regulator of the mTORC1 pathway, AMPK may be a candidate for the induction of spinal Rheb expression after repeated intrathecal morphine treatment.

We used metformin, an activator of AMPK, and injected it intraperitoneally to observe its effect on the development of morphine-induced tolerance. During the development of morphine-induced tolerance, reduction in morphine-induced antinociceptive effect was significantly mitigated by coadministration of metformin (fig. 7, A and B), retaining approximately 40% of the maximum possible effect on day 5 in the morphine + metformin group (fig. 7C, maximum possible effect on day 5: 39.51 ± 7.40% in morphine + metformin group *vs.* 15.58 ± 5.79% in morphine group, $P < 0.0001$, $n = 6$). The maximum possible effect on day 5 was reduced to approximately 83% in the morphine group in comparison with day 1, and coadministration of metformin partially prevented the decrease, resulting in approximately 60% of morphine-induced maximum possible effect (fig. 7D; change in maximum possible effect: −59.73 ± 6.47% in morphine + metformin group *vs.* −83.46 ± 5.03% in morphine group, $P < 0.0001$, $P < 0.0001$, $n = 6$).

Additionally, we observed that phosphorylation of spinal AMPK was decreased significantly after repeated intrathecal morphine treatment (fig. 7E; phosphorylation level: 2.08 ± 0.29 in saline group *vs.* 1.17 ± 0.35 in morphine group, $P = 0.0006$, $n = 6$). Activation of AMPK with intraperitoneal metformin effectively prevented the chronic morphine-induced downregulation of spinal AMPK phosphorylation (fig. 7F; phosphorylation level: 0.07 ± 0.087 in morphine group *vs.* 0.76 ± 0.63 in morphine + metformin group, $P = 0.0246$, $n = 6$). Interestingly, metformin significantly inhibited the upregulation of chronic morphine-induced spinal Rheb (fig. 7G; Rheb level: 0.99 ± 0.70 in morphine group *vs.* 0.27 ± 0.21 in morphine + metformin group, $P = 0.0145$, $n = 7$). Furthermore, coadministration of metformin decreased the level of phosphorylation of spinal mTOR (fig. 7H; phosphorylation level: 1.07 ± 0.61 in morphine group *vs.* 0.29 ± 0.13 in morphine + metformin group, $P = 0.005$, $n = 6$), 4EBP1 (fig. 7I; phosphorylation level: 1.0 ± 0.18 in morphine group *vs.* 0.70 ± 0.20 in morphine + metformin group, $P = 0.0204$, $n = 6$), and S6 (fig. 7J; phosphorylation level: 1.0 ± 0.11 in morphine

Downloaded from http://asa2.silverchair.com/anesthesiology/article-pdf/140/4/786/701885/20240400.0-00022.pdf by guest on 20 March 2024

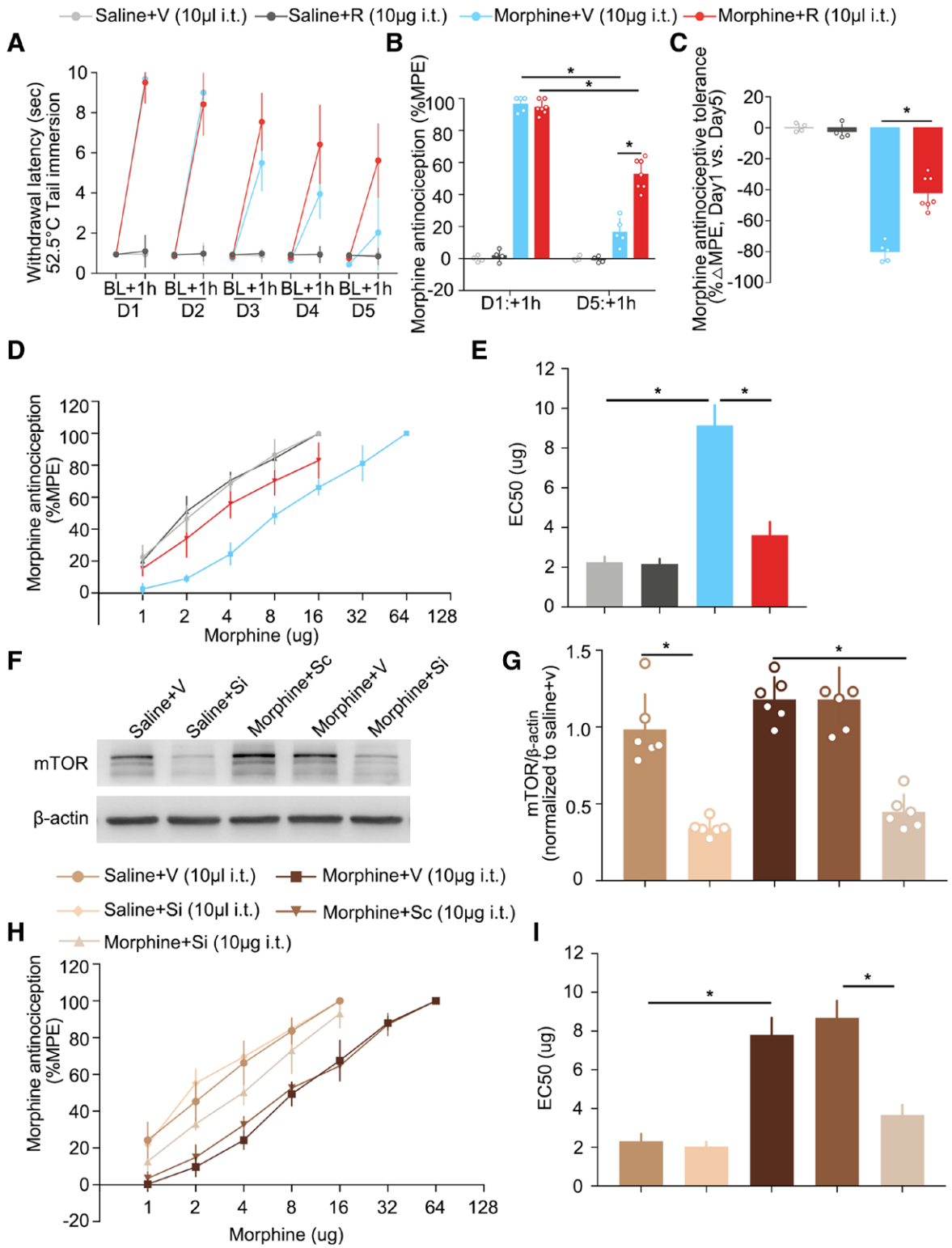

Fig. 6. Inhibition of mTOR prevents the development of morphine-induced tolerance. (*A*) Daily nociceptive behavior and morphine antinociception during a 5-day chronic morphine schedule (10 μg in 10 μl of saline, intrathecal, twice daily). The animals were pretreated with vehicle (V, 10 μl of 1 ‰ dimethyl sulfoxide [DMSO]) or rapamycin (R, 10 μg in 10 μl of 1 ‰ DMSO) intrathecally 30 min before morphine intrathecal injection. (*B*) Antinociceptive tolerance: maximum possible effect (MPE) for morphine antinociception from the *(Continued)*

Downloaded from http://asa2.silverchair.com/anesthesiology/article-pdf/140/4/786/701885/20240400.0-00022.pdf by guest on 20 March 2024

group *vs.* 0.47 ± 0.15 in morphine + metformin group, $P < 0.0001$, n = 6). Double-immunofluorescence staining results revealed that the localization of p-AMPK overlapped with that of neuronal markers NeuN (fig. 7L) and Rheb (fig. 7K), consistent with the expression patterns of Rheb and p-S6. These results demonstrate that Rheb is regulated by the endogenous level and/or activity of AMPK, possibly in a phosphorylation manner, thereby serving as an indispensable molecular switch for bidirectional regulation of morphine efficacy and tolerance.

Discussion

This study showed that chronic morphine treatment decreased the phosphorylation of spinal AMPK and increased the expression of spinal Rheb, leading to the activation of spinal mTOR signaling, which underlies the development of morphine-induced tolerance. Elevation of AMPK levels and spinal *Rheb* knockout alleviated these effects. Conversely, overexpression of *Rheb* in the spinal cord had the opposite effects. Based on these results and those of our previous study,[12] we propose that the small GTPase Rheb is involved in the AMPK–Rheb–mTOR signaling pathway and acts as a key endogenous switch axis for bidirectional regulation of the development and maintenance of morphine-induced tolerance in the spinal dorsal horn. To this end, targeting spinal Rheb may present a new therapeutic strategy for potentially preventing and even reversing chronic morphine-induced tolerance.

Previous studies have demonstrated that Rheb mRNA levels are significantly increased 2 h after carrageenan injection during hypersensitivity induction by peripheral inflammation[30] and are modulated in a morphine-induced conditioned manner.[31] However, its potential roles in morphine tolerance remain unknown. We demonstrated that *Rheb* overexpression impaired intrathecal morphine-induced analgesia, as evidenced by the phenotype of *Rheb* S16H mice observed in this study and the opposite effects detected by its deletion in excitatory neurons in the spinal cord. Chronic morphine treatment induces antinociceptive tolerance[32]; hence, our finding on the profound increase in spinal Rheb after repeated morphine exposure indicates that Rheb plays a vital role in pain modulation and the development of chronic morphine-induced tolerance. Rheb mRNA levels did not change after chronic morphine treatment in this study. The increase in Rheb protein may be attributed to a reduction in degradation or an enhancement in protein translation. These findings provide unequivocal evidence for the causal link between endogenous Rheb-dependent signaling and morphine-induced analgesia.

As a negative regulator of the Rheb-mTOR signaling pathway, activated AMPK promotes the inhibition of Rheb, subsequently affecting mTORC1 activity. Therefore, AMPK is likely responsible for the increase in spinal Rheb during the development of morphine-induced tolerance. In contrast to the results of previous studies,[15,33,34] we showed that AMPK-Rheb signaling in a subset of spinal excitatory neurons likely accounts for the development of morphine-induced antinociceptive tolerance. Activation of AMPK suppresses neuroinflammation and ameliorates bone cancer pain[35] and other types of pathologic pain.[36] In addition to modulating pain transduction, AMPK-modulated Rheb expression has been reported in functional dyspepsia treatment at the protein and mRNA levels.[37] These observations suggest that AMPK is a potent negative regulator of Rheb expression. In our study, chronic morphine exposure induced the inhibition of spinal AMPK activity (as evidenced by its lowered phosphorylation levels), disinhibiting spinal Rheb expression, which in turn activated mTOR signaling. Metformin activated AMPK to counteract the increase in Rheb levels induced by morphine, thereby mitigating its tolerance. Previous studies have demonstrated the antinociceptive effect of metformin in rodent pain models; metformin relieved spinal nerve ligation–induced tactile allodynia in rats and mice by activating AMPK and inhibiting the mTORC1 pathway.[38,39] Additionally, metformin prevented tactile allodynia in other neuropathic pain models, such as those of spinal cord injury[40] and bortezomib-, paclitaxel-, and cisplatin-induced hyperalgesia[41,42] in rodents. Activation of AMPK reduced morphine tolerance by inhibiting microglial-mediated neuroinflammation.[15,33] These results demonstrate that AMPK is an important target in the regulation of pain by metformin, although it has many other AMPK-independent effectors.

mTORC1 signaling is known to control growth by balancing anabolic processes, such as protein, lipid, and nucleotide synthesis. Dysregulation of mTORC1 signaling leads to abnormalities in many diseases, including cancer, diabetes, neurodegeneration conditions, and epilepsy. Although rapamycin, a potent inhibitor of mTORC1, has demonstrated efficacy, it may also have unexpected off-target effects owing to the broad involvement of mTORC1 signaling in the synthesis of various proteins involved in many physiologic and pathologic processes. In this study, we demonstrated that Rheb regulates the levels of key protein substrates specifically associated with morphine-dependent tolerance. Decreased expression

Fig. 6. *(Continued)* first administration (day 1, + 1 h) compared to the last administration (day 5, + 1 h). (*C*) Percentage of change for each subject. (*D*) Dose–response curve on day 6 after a 5-day chronic morphine schedule. (*E*) EC_{50} for each group. (*F*) Immunoblotting of the spinal dorsal horn with anti-mTOR antibody in mice administered with saline and morphine pretreated with vehicle (V), mTOR siRNA (Si), or scramble RNA (Sc). (*G*) Respective quantification of mTOR. (*H*) Dose–response curve on day 6 after a 5-day chronic morphine schedule. (*I*) EC_{50} for each group (n = 6 mice in each group). The data are presented as means ± SD by repeated-measures two-way ANOVA + Bonferroni (*B*) or one-way ANOVA + Bonferroni (*C*, *E*, *G*, *I*). **P* < 0.05. The overlaid points are individual animal scores. BL, baseline; +1 h, 1 h after morphine injection; D1, on Day 1.

Downloaded from http://asa2.silverchair.com/anesthesiology/article-pdf/140/4/786/701885/20240400.0-00022.pdf by guest on 20 March 2024

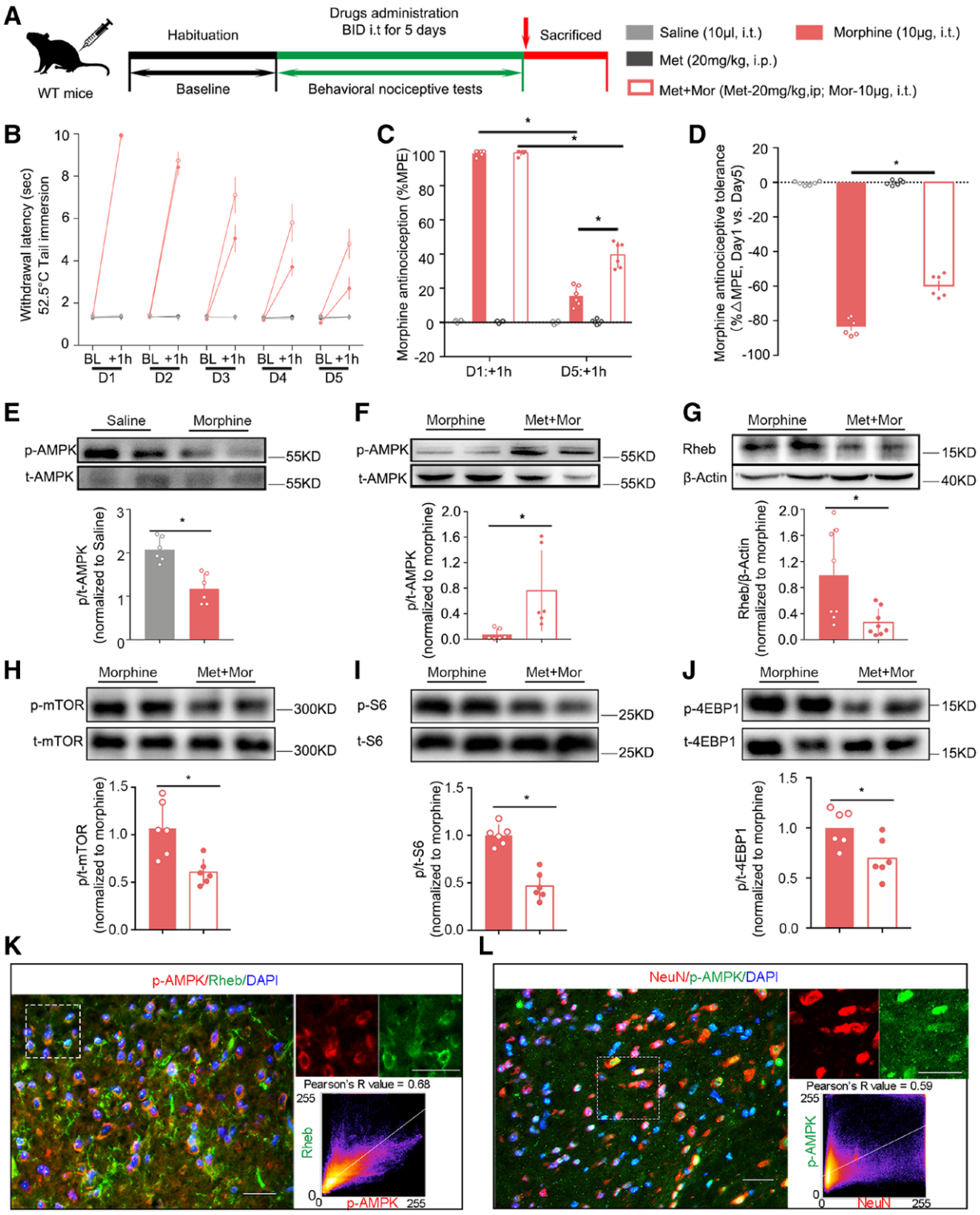

Fig. 7. Metformin prevents opiate tolerance by preventing Rheb induction. (*A*) Timeline of the experimental procedure. (*B*) Daily nociceptive behavior and morphine antinociception during a 5-day chronic morphine schedule (10 μg in 10 μl of saline, intrathecal, twice daily). Saline or metformin (200 mg/kg, ip, 20 μg/μl in saline) was administered 30 min before morphine intrathecal injection. (*C*) Antinociceptive tolerance: maximum possible effect for morphine antinociception from the first administration (day 1, 1 h after morphine injection) compared to the last administration (day 5, 1 h after morphine injection). (*D*) Percentage of change in each subject. (*E* to *G*) Immunoblotting of *(Continued)*

Downloaded from http://asa2.silverchair.com/anesthesiology/article-pdf/140/4/786/701885/20240400.0-00022.pdf by guest on 20 March 2024

Fig. 7. *(Continued)* the spinal dorsal horn with anti-p/t-AMPK, Rheb, and β-actin antibodies. (*H* to *J*) Immunoblotting of the spinal dorsal horn with anti-p/t-mTOR, p/t-S6, and p/t-4EBP1 antibodies. (*K*) Immunofluorescence double labeling of p-AMPK (*red*) with Rheb (*green*). The *top panels* are enlarged in two separate boxes with single images included in the picture. *Scale bars*, 50 μm (*top*) and 20 μm (*bottom*). The Pearson's *R* value of colocalization was quantified. (*L*) Immunofluorescence double labeling of p-AMPK (green) with NeuN (red). The *top panels* are enlarged in two separate boxes with single images included in the picture. *Scale bars*, 50 μm (*top*) and 20 μm (*bottom*). The Pearson's *R* value of colocalization was quantified. The data are presented as means ± SD by repeated-measures two-way ANOVA + Bonferroni (*C*), one-way ANOVA + Bonferroni (*D*), and unpaired two-tailed Student's *t* test (*E* to *J*). **P* < 0.05.

of Rheb in excitatory neurons may potentiate morphine-induced acute analgesia and reduce chronic morphine-induced antinociceptive tolerance. Conversely, overexpression of Rheb impaired the antinociceptive effect of acute morphine. These completely opposite effects provided a proof of concept for the rational use of Rheb as an ideal drug target, as it is uniquely situated immediately upstream of the mTORC1 signaling cascade, thus affecting a subset of specific key proteins critical for morphine-induced tolerance/hyperalgesia.

Morphine increases the release of excitatory peptides[43] and induces neuroplastic changes, which underlie spinal excitability reflected as thermal and tactile hypersensitivity to peripheral stimuli.[9] Notably, Rheb regulates the expression of excitatory amino acid transporter 4 and limited extracellular glutamate levels,[44] whereas a loss of its downstream effector in excitatory neurons reduces evoked excitatory postsynaptic current amplitudes.[45] Opioid-induced plasticity has been reported in both acute and chronic morphine-induced analgesic tolerance.[46] The activation of AMPK signaling inhibited spinal synaptic plasticity, alleviating acute pain.[47] In persistent postsurgical pain, indirect AMPK activators prevent long-term neuronal plasticity.[48] Additionally, spinal Rheb-mTOR signaling regulates spinal sensitization and inhibition, because blocking spinal mTOR could attenuate inflammation-induced thermal and tactile hypersensitivity.[30] mTOR signaling in the spinal cord is required for neuronal plasticity and behavioral hypersensitivity associated with neuropathy, neuronal circuits of facilitated pain processing in inflammation-induced hyperalgesia,[49] and the development and maintenance of bone cancer–induced pain hypersensitivities.[50] Our experiments showing site- and cell-specific overexpression or knockout of *Rheb* in transgenic mice provided compelling evidence that Rheb is necessary for bridging AMPK and mTOR-dependent protein translation in spinal excitatory neurons to causally underpin the development of morphine tolerance, hyperalgesia, and possibly other sensory maladaptations. Nevertheless, the data from this study cannot absolutely rule out the supraspinal impact of Rheb on morphine tolerance, which is one of the limitations of this study.

Overall, we propose a new working model in which the AMPK-Rheb-mTOR signaling pathway in the dorsal horn excitatory neurons regulates morphine tolerance. After long-term opioid administration, chronic morphine decreases the phosphorylation of spinal AMPK, subsequently disinhibiting the expression of spinal Rheb. This is followed by activation of downstream mTOR signaling to stimulate S6K and 4E-BP activities, resulting in the initiation of mRNA translation and adaptive changes in protein translation in the dorsal horn.[12] Therefore, Rheb signaling is a key regulator of the aberrant plasticity of nociceptive circuits and adaptation during chronic morphine exposure. In addition to opioid-induced tolerance and hyperalgesia, patients with neuropathic and inflammatory pain may benefit from Rheb inhibition. Thus, intrathecal use of mTOR inhibitors or metformin clinically may have additional benefits, such as antinociception and anti-tolerance, and serve as a potentially superior strategy in managing opioid-induced tolerance.

Acknowledgments

It is with the deepest gratitude that the authors thank Paul F. Worley, Ph.D., (Solomon H. Snyder Department of Neuroscience, Johns Hopkins University School of Medicine, Baltimore, Maryland) for his kindness and the invaluable transgenic mice. They also thank Editage for English language editing.

Research Support

Supported by the General Program of the National Natural Science Foundation of China (Beijing, China) under grant Nos. 82171486 (to Dr. Xu) and 82171262 (to Dr. Jiang); the Shanghai Natural Science Foundation (Shanghai, China) under grant No. 21ZR1448400 (to Dr. Xu); the Key Project of Medical Engineering Intersection of Shanghai Jiaotong University (Shanghai, China) under grant No. YG2021ZD23 (to Dr. Xu); the Incubation Project of Shanghai Sixth People's Hospital (Shanghai, China) under grant No. YNMS202114 (to Dr. Xu); the Shanghai Sailing Program (Shanghai, China) under grant No. 21YF1434200 (to Dr. Wang); and the Youth Program of the National Natural Science Foundation of China under grant Nos. 82001455 (to Dr. Du) and 82201366 (to Dr. Ma).

Competing Interests

The authors declare no competing interests.

Correspondence

Address correspondence to Dr. Xu: Shanghai Sixth People's Hospital, Shanghai Jiao Tong University, 600 Yi Shan Road, Shanghai 200233, China. balor@sjtu.edu.cn

Downloaded from http://asa2.silverchair.com/anesthesiology/article-pdf/140/4/786/701885/20240400.0-00022.pdf by guest on 20 March 2024

Supplemental Digital Content

Supplementary Content 1. Validation of transgenic mice, https://links.lww.com/ALN/D418
Supplementary Content 2. Modulation of spinal Rheb expression in female mice, https://links.lww.com/ALN/D418
Supplementary Content 3. Validation of the morphine-induced tolerance model, https://links.lww.com/ALN/D418
Supplementary Content 4. Full-length Western blotting images, https://links.lww.com/ALN/D419

References

1. Dahlhamer J, Lucas J, Zelaya C, et al.: Prevalence of chronic pain and high-impact chronic pain among adults—United States, 2016. MMWR Morb Mortal Wkly Rep 2018; 67:1001–6
2. Eisenberg E, McNicol ED, Carr DB: Efficacy and safety of opioid agonists in the treatment of neuropathic pain of nonmalignant origin: Systematic review and meta-analysis of randomized controlled trials. JAMA 2005; 293:3043–52
3. Chu LF, Angst MS, Clark D: Opioid-induced hyperalgesia in humans: Molecular mechanisms and clinical considerations. Clin J Pain 2008; 24:479–96
4. Christie MJ: Cellular neuroadaptations to chronic opioids: Tolerance, withdrawal and addiction. Br J Pharmacol 2008; 154:384–96
5. Szabo I, Chen XH, Xin L, et al.: Heterologous desensitization of opioid receptors by chemokines inhibits chemotaxis and enhances the perception of pain. Proc Natl Acad Sci USA 2002; 99:10276–81
6. Chakrabarti S, Liu NJ, Gintzler AR: Formation of mu-/kappa-opioid receptor heterodimer is sex-dependent and mediates female-specific opioid analgesia. Proc Natl Acad Sci USA 2010; 107:20115–9
7. Gardell LR, Wang R, Burgess SE, et al.: Sustained morphine exposure induces a spinal dynorphin-dependent enhancement of excitatory transmitter release from primary afferent fibers. J Neurosci 2002; 22:6747–55
8. Vanderah TW, Suenaga NM, Ossipov MH, Malan TP Jr, Lai J, Porreca F: Tonic descending facilitation from the rostral ventromedial medulla mediates opioid-induced abnormal pain and antinociceptive tolerance. J Neurosci 2001; 21:279–86
9. Vera-Portocarrero LP, Zhang ET, King T, et al.: Spinal NK-1 receptor expressing neurons mediate opioid-induced hyperalgesia and antinociceptive tolerance via activation of descending pathways. Pain 2007; 129:35–45
10. Merighi S, Gessi S,Varani K, Fazzi D, Stefanelli A, Borea PA: Morphine mediates a proinflammatory phenotype via mu-opioid receptor-PKCvarepsilon-Akt-ERK1/2 signaling pathway in activated microglial cells. Biochem Pharmacol 2013; 86:487–96
11. Sanchez-Blazquez P, Rodriguez-Munoz M, Garzon J: Mu-opioid receptors transiently activate the Akt-nNOS pathway to produce sustained potentiation of PKC-mediated NMDAR-CaMKII signaling. PLoS One 2010; 5:e11278
12. Xu JT, Zhao JY, Zhao X, et al.: Opioid receptor-triggered spinal mTORC1 activation contributes to morphine tolerance and hyperalgesia. J Clin Invest 2014; 124:592–603
13. Zou J, Zhou L, Du XX, et al.: Rheb1 is required for mTORC1 and myelination in postnatal brain development. Dev Cell 2011; 20:97–108
14. Zheng M, Wang YH, Wu XN, et al.: Inactivation of Rheb by PRAK-mediated phosphorylation is essential for energy-depletion–induced suppression of mTORC1. Nat Cell Biol 2011; 13:263–72
15. Pan Y, Sun X, Jiang L, et al.: Metformin reduces morphine tolerance by inhibiting microglial-mediated neuroinflammation. J Neuroinflammation 2016; 13:294
16. Zou J, Zhou LA, Du XX, et al.: Rheb1 is required for mTORC1 and myelination in postnatal brain development. Dev Cell 2011; 20:97–108
17. Bailey RM, Rozenberg A, Gray SJ: Comparison of high-dose intracisterna magna and lumbar puncture intrathecal delivery of AAV9 in mice to treat neuropathies. Brain Res 2020; 1739:146832
18. Bohn LM, Gainetdinov RR, Lin FT, Lefkowitz RJ, Caron MG: Mu-opioid receptor desensitization by beta-arrestin-2 determines morphine tolerance but not dependence. Nature 2000; 408:720–3
19. Bohn LM, Lefkowitz RJ, Gainetdinov RR, Peppel K, Caron MG, Lin FT: Enhanced morphine analgesia in mice lacking beta-arrestin 2. Science 1999; 286:2495–8
20. Xu H, Xu T, Ma X, Jiang W: Involvement of neuronal TGF-beta activated kinase 1 in the development of tolerance to morphine-induced antinociception in rat spinal cord. Br J Pharmacol 2015; 172:2892–904
21. Eidson LN, Inoue K, Young LJ, Tansey MG, Murphy AZ: Toll-like receptor 4 mediates morphine-induced neuroinflammation and tolerance via soluble tumor necrosis factor signaling. Neuropsychopharmacology 2017; 42:661–70
22. Faul F, Erdfelder E, Lang AG, Buchner A: G*Power 3: A flexible statistical power analysis program for the social, behavioral, and biomedical sciences. Behav Res Methods 2007; 39:175–91
23. Huang M, Luo L, Zhang Y, et al.: Metabotropic glutamate receptor 5 signalling induced NMDA receptor subunits alterations during the development of morphine-induced antinociceptive tolerance in mouse cortex. Biomed Pharmacother 2019; 110:717–26

Downloaded from http://asa2.silverchair.com/anesthesiology/article-pdf/140/4/786/701885/20240400.0-00022.pdf by guest on 20 March 2024

24. Laplante M, Sabatini DM: mTOR signaling in growth control and disease. Cell 2012; 149:274–93
25. Hay N, Sonenberg N: Upstream and downstream of mTOR. Genes Dev 2004; 18:1926–45
26. Costa-Mattioli M, Sossin WS, Klann E, Sonenberg N: Translational control of long-lasting synaptic plasticity and memory. Neuron 2009; 61:10–26
27. Srivastava IN, Shperdheja J, Baybis M, Ferguson T, Crino PB: mTOR pathway inhibition prevents neuroinflammation and neuronal death in a mouse model of cerebral palsy. Neurobiol Dis 2016; 85:144–54
28. Xie L, Sun F, Wang J, et al.: mTOR signaling inhibition modulates macrophage/microglia-mediated neuroinflammation and secondary injury via regulatory T cells after focal ischemia. J Immunol 2014; 192:6009–19
29. Zheng XF, Florentino D, Chen J, Crabtree GR, Schreiber SL: TOR kinase domains are required for two distinct functions, only one of which is inhibited by rapamycin. Cell 1995; 82:121–30
30. Norsted Gregory E, Codeluppi S, Gregory JA, Steinauer J, Svensson CI: Mammalian target of rapamycin in spinal cord neurons mediates hypersensitivity induced by peripheral inflammation. Neuroscience 2010; 169:1392–402
31. Martinez-Rivera FJ, Martinez NA, Martinez M, Ayala-Pagan RN, Silva WI, Barreto-Estrada JL: Neuroplasticity transcript profile of the ventral striatum in the extinction of opioid-induced conditioned place preference. Neurobiol Learn Mem 2019; 163:107031
32. Dogrul A, Bilsky EJ, Ossipov MH, Lai J, Porreca F: Spinal L-type calcium channel blockade abolishes opioid-induced sensory hypersensitivity and antinociceptive tolerance. Anesth Analg 2005; 101:1730–5
33. Han Y, Jiang C, Tang J, et al.: Resveratrol reduces morphine tolerance by inhibiting microglial activation via AMPK signalling. Eur J Pain 2014; 18:1458–70
34. Zhang Y, Tao GJ, Hu L, et al.: Lidocaine alleviates morphine tolerance via AMPK-SOCS3-dependent neuroinflammation suppression in the spinal cord. J Neuroinflammation 2017; 14:211
35. Song H, Han Y, Pan C, et al.: Activation of adenosine monophosphate-activated protein kinase suppresses neuroinflammation and ameliorates bone cancer pain: Involvement of inhibition on mitogen-activated protein kinase. Anesthesiology 2015; 123:1170–85
36. Asiedu MN, Dussor G, Price TJ: Targeting AMPK for the alleviation of pathological pain. Exp Suppl 2016; 107:257–85
37. Tang L, Zeng Y, Li L, et al.: Electroacupuncture upregulated ghrelin in rats with functional dyspepsia via AMPK/TSC2/Rheb-mediated mTOR inhibition. Dig Dis Sci 2019; 65:1689–99
38. Melemedjian OK, Asiedu MN, Tillu DV, et al.: Targeting adenosine monophosphate-activated protein kinase (AMPK) in preclinical models reveals a potential mechanism for the treatment of neuropathic pain. Mol Pain 2011; 7:70
39. Inoki K, Kim J, Guan KL: AMPK and mTOR in cellular energy homeostasis and drug targets. Annu Rev Pharmacol Toxicol 2012; 52:381–400
40. Liu YT, Li JM, Li H, et al.: AMP-activated protein kinase activation in dorsal root ganglion suppresses mTOR/p70S6K signaling and alleviates painful radiculopathies in lumbar disc herniation rat model. Spine 2019; 44:E865–72
41. Mao-Ying QL, Kavelaars A, Krukowski K, et al.: The anti-diabetic drug metformin protects against chemotherapy-induced peripheral neuropathy in a mouse model. PLoS One 2014; 9:e100701
42. Ludman T, Melemedjian OK: Bortezomib and metformin opposingly regulate the expression of hypoxia-inducible factor alpha and the consequent development of chemotherapy-induced painful peripheral neuropathy. Mol Pain 2019; 15:1744806919850043
43. Crain SM, Shen KF: Antagonists of excitatory opioid receptor functions enhance morphine's analgesic potency and attenuate opioid tolerance/dependence liability. Pain 2000; 84:121–31
44. Jiang NW, Wang DJ, Xie YJ, et al.: Downregulation of glutamate transporter EAAT4 by conditional knockout of Rheb1 in cerebellar Purkinje cells. Cerebellum 2016; 15:314–21
45. Angliker N, Burri M, Zaichuk M, Fritschy JM, Ruegg MA: mTORC1 and mTORC2 have largely distinct functions in Purkinje cells. Eur J Neurosci 2015; 42:2595–612
46. Taylor BK: Insights into morphine-induced plasticity and spinal tolerance. Pain 2005; 114:1–2
47. Ling YZ, Li ZY, Ou-Yang HD, et al.: The inhibition of spinal synaptic plasticity mediated by activation of AMP-activated protein kinase signaling alleviates the acute pain induced by oxaliplatin. Exp Neurol 2017; 288:85–93
48. Inyang KE, Burton MD, Szabo-Pardi T, et al.: Indirect AMP-activated protein kinase activators prevent incision-induced hyperalgesia and block hyperalgesic priming, whereas positive allosteric modulators block only priming in mice. J Pharmacol Exp Ther 2019; 371:138–50
49. Xu Q, Fitzsimmons B, Steinauer J, et al.: Spinal phosphinositide 3-kinase-Akt-mammalian target of rapamycin signaling cascades in inflammation-induced hyperalgesia. J Neurosci 2011; 31:2113–24
50. Shih MH, Kao SC, Wang W, Yaster M, Tao YX: Spinal cord NMDA receptor-mediated activation of mammalian target of rapamycin is required for the development and maintenance of bone cancer-induced pain hypersensitivities in rats. J Pain 2012; 13:338–49

Downloaded from http://asa2.silverchair.com/anesthesiology/article-pdf/140/4/786/701885/20240400.0-00022.pdf by guest on 20 March 2024